Journal of Geophysical Research: Planets

RESEARCH ARTICLE
10.1029/2018JE005540

The Effect of Mars-Relevant Soil Analogs on the Water Uptake of Magnesium Perchlorate and Implications for the Near-Surface of Mars

K. M. Primm[1,2], R. V. Gough[1,2], J. Wong[2], E. G. Rivera-Valentin[3], G. M. Martinez[4], J. V. Hogancamp[5], P. D. Archer[5], D. W. Ming[5], and M. A. Tolbert[1,2]

[1]Cooperative Institute for Research in Environmental Sciences, University of Colorado, Boulder, CO, USA, [2]Department of Chemistry and Biochemistry, University of Colorado, Boulder, CO, USA, [3]Lunar and Planetary Institute, Universities Space Research Association, Houston, TX, USA, [4]Department of Climate and Space Sciences and Engineering, University of Michigan, Ann Arbor, MI, USA, [5]Jacobs at NASA Johnson Space Center, Houston, TX, USA

Key Points:
- This paper discusses the water uptake and release of Martian salts, mixed with regolith analogs
- The DRH, ERH, and ice RH of magnesium perchlorate were not affected by Mars-relevant regolith analogs
- Brines are predicted in the subsurface at PHX site, but not at Gale Crater

Supporting Information:
- Supporting Information S1

Correspondence to:
M. A. Tolbert,
margaret.tolbert@colorado.edu

Citation:
Primm, K. M., Gough, R. V., Wong, J., Rivera-Valentin, E. G., Martinez, G. M., Hogancamp, J. V., et al. (2018). The effect of Mars-relevant soil analogs on the water uptake of magnesium perchlorate and implications for the near-surface of Mars. *Journal of Geophysical Research: Planets*, *123*, 2076–2088. https://doi.org/10.1029/2018JE005540

Received 19 JAN 2018
Accepted 20 JUL 2018
Accepted article online 6 AUG 2018
Published online 23 AUG 2018

Abstract The water uptake and release by perchlorate salts have been well studied since the first in situ identification of such salts in the Martian soil by the Phoenix mission in 2008. However, there have been few studies on the effect of the insoluble regolith minerals on the interaction of perchlorate with water vapor. In this work, we investigate the impact of a Mars-relevant mineral, montmorillonite, and a Mars soil analog, Mojave Mars Simulant (MMS), on the deliquescence (transition from dry crystalline to aqueous via water vapor absorption), ice formation, and efflorescence (transition from aqueous to dry crystalline via loss of water) of pure magnesium perchlorate. We studied mixtures of magnesium perchlorate hexahydrate with either montmorillonite or MMS. Although montmorillonite and MMS are materials that may serve as nuclei for either ice nucleation or salt efflorescence, we find that these soil analogs did not affect the phase transitions of magnesium perchlorate. The salt-mineral mixture behaved similarly, within estimated uncertainties, to pure magnesium perchlorate in all cases. Experiments were performed in both N_2 and CO_2 atmospheres, with no detectable difference. We use data from the Mars Science Laboratory Rover Environmental Monitoring Station instrument and the Phoenix Thermal and Electrical Conductivity Probe, as well as modeling of the shallow subsurface, to determine the likelihood of these perchlorate phase transitions occurring at Gale Crater and the northern arctic plains (Vastitas Borealis). We find that aqueous solutions are predicted in the shallow subsurface of the Phoenix landing site, but not predicted at Gale Crater.

Plain Language Summary Most previous studies on Mars-relevant salts have looked at the water uptake and release of the pure salts, but few have looked at the effect that insoluble minerals might have on the water uptake and release. This is an important potential effect because the surface of Mars is mainly composed of (~99%) mineral dust and we might not be accurately predicting if liquid solutions are possible on Mars today. However, this study shows that a Mars-relevant mineral (montmorillonite) and a Mars surface analog (Mojave Mars Simulant) did not have a significant effect on the water uptake of magnesium perchlorate. In addition, the Phoenix landing site is more favorable to support liquid solutions of magnesium perchlorate, rather than Gale Crater (Curiosity's current site).

1. Introduction

The perchlorate anion (ClO_4^-) has been found or inferred at ~0.5 wt % at several locations on Mars: at the Phoenix (PHX) landing site (Hecht et al., 2009), in soil samples along the Mars Science Laboratory (MSL) traverse at Gale Crater (Glavin et al., 2013), at recurring slope lineae locations (Ojha et al., 2015), and potentially at the Viking landing sites (Navarro-González et al., 2010). Perchlorate salts have unique properties that provide multiple potential mechanisms for the formation of liquid water on present-day Mars. Perchlorates can depress the freezing point of water to very low eutectic temperatures (~200 K; Chevrier et al., 2009; Marion et al., 2010; Pestova et al., 2005). Additionally, perchlorate salts can absorb atmospheric water vapor and deliquesce into a liquid solution (Fischer et al., 2014; Gough et al., 2011, 2014; Nuding et al., 2014; Zorzano et al., 2009).

Deliquescence is the transition that occurs when a dry crystalline particle absorbs water vapor and turns into an aqueous droplet, while efflorescence is the opposite phase transition where an aqueous drop loses water

and transitions to a dry crystalline particle. Deliquescence occurs when the relative humidity (RH) with respect to liquid ($RH_{(l)}$) surpasses the deliquescence RH (DRH) of a salt at a given temperature (above its eutectic value) and leads to the formation of a saturated salt solution. The eutectic temperature of a salt mixture is defined as the lowest temperature at which aqueous solutions are stable. If a salt has a low eutectic temperature, as do many perchlorate salts (Chevrier et al., 2009), there is a very large temperature range over which the salt can deliquesce and form a liquid solution, using only water vapor as the source. Perchlorate salts often have efflorescence RH (ERH) values that are far below the DRH (Gough et al., 2011; Nuding et al., 2014). The hysteresis occurring between the DRH and ERH is due to the kinetic inhibition of nucleation and can extend the duration of a potential brine (Reid & Sayer, 2003).

Although the freezing of Mars-relevant salts has been studied, the relative humidities at which they freeze over a range of conditions relevant to Mars have not been studied. The ability of an environment to produce ice can be quantified by S_{ice}, defined as the partial pressure of water vapor over the equilibrium saturated vapor pressure of water over ice at a given temperature. It is thermodynamically predicted in many models that ice should begin to form when $S_{ice} = 1$; however, because critical clusters of ice must form for ice to grow, supersaturation with respect to ice (i.e., S_{ice} values greater than unity) are often required before freezing can begin. We have recently found that S_{ice} values $\geq$1.3 are required for a perchlorate brine droplet to freeze (Primm et al., 2017).

Many recent studies have examined the deliquescence, efflorescence, or freezing of pure perchlorate salts or brines (Fischer et al., 2014, 2016; Gough et al., 2011; Nikolakakos & Whiteway, 2015; Nuding et al., 2014; Primm et al., 2017; Toner et al., 2015). The low-temperature phase transition behavior of many pure perchlorates is therefore fairly well established. However, because the surface of Mars is primarily (~99%) minerals and dust (Ehlmann & Edwards, 2014), it is conceivable that the presence of these minerals in contact with, or in the interior of, a salt grain would affect the interactions of the salt with water. The mineral could affect the uptake of atmospheric water vapor by the salt due to competition for water molecules. In contrast to deliquescence, efflorescence and ice formation are nucleation processes and may thus be affected when insoluble nuclei are introduced and provide for an external nucleation species and prevent supercooling or supersaturation.

In the atmospheric chemistry literature, studies in the last decade have shown that mineral dust serves as an excellent ice nucleus (i.e., forms ice at low relative humidities) (J. Han & Martin, 1999; Hoose & Möhler, 2012; Pant et al., 2006). In fact, field studies show that ice residual particles (particles remaining after atmospheric ice are evaporated) are most often aluminosilicate (mineral dust) in nature (Cziczo et al., 2013). In addition, laboratory studies have shown that the minerals hematite and corundum increase the ERH of ammonium nitrate and ammonium sulfate (J. H. Han et al., 2001; Martin et al., 2001). Thus, minerals relevant to Earth's atmosphere have been shown to be efficient ice nuclei for both ice and salt crystal nucleation. If minerals behave similarly when mixed with perchlorates, the presence of minerals could substantially alter the brine stability conditions on Mars. However, only a few studies have examined the effect of the Martian regolith on perchlorate phase transitions involving nucleation. Nikolakakos and Whiteway (2018) studied the deliquescence of magnesium perchlorate mixed with chabazite (a Mars-relevant mineral) and quartz sand and found that the DRH of the magnesium perchlorate was not affected by the adsorption of water by the mineral. In addition, Toner et al. (2014) found that JSC Mars-1 did not promote salt crystallization upon cooling. Here we experimentally examine the full range of phase transitions (deliquescence, efflorescence, and ice formation) for perchlorate-mineral mixtures in order to understand the complete interaction between water vapor, hygroscopic salts, and minerals on Mars and the potential for small scale liquid brines.

2. Experimental Methods

2.1. Sample Preparation

Equal masses of magnesium perchlorate hexahydrate and either montmorillonite or Mojave Mars Simulant (MMS) were mixed in high-performance liquid chromatography grade water. This ratio was selected because it gave the most reliable Raman spectral signal of each component (Figure S1 in the supporting information). Magnesium perchlorate hexahydrate was obtained from Sigma Aldrich (99% purity), sodium montmorillonite (SWy-2) from the Clay Mineral Society, and MMS from National Aeronautics and Space Administration Jet Propulsion Laboratory (G. Peters). Montmorillonite has a bimodal spherical diameter of 60 and 250 nm (Assemi et al., 2015), and the MMS that was used here was MMS dust with a grain size of $\leq$0.4 mm (Peters

Table 1
Chemical Composition of Mojave Mars Simulant (MMS) Whole Rock Samples (Peters et al., 2008)

Concentration (wt %)	MMS
SiO_2	49.4
TiO_2	1.09
Al_2O_3	17.1
Cr_2O_3	0.05
Fe_2O_3	10.87
MnO	0.17
MgO	6.08
CaO	10.45
Na_2O	3.28
K_2O	0.48
P_2O_5	0.17
SO_3	0.10
LOI (loss on ignition)[a]	3.39

[a]LOI typically consists of Cl, SO_3, and H_2O.

et al., 2008), and a unimodal diameter of 30.21 μm was determined. The small size of the montmorillonite ensured that it remained in colloidal form during nebulization, resulting in 1:1 montmorillonite: salt mixtures in the particle. However, when mixing the magnesium perchlorate with the MMS in water, a significant amount of large MMS grains settled out. To create a more representative 1:1 ratio of salt to MMS, a known mass of MMS was placed into a known amount of water. After inverting and shaking the mixture, the larger particles of MMS settled out (around 10 min) and the slurry of dissolved MMS was decanted to separate. Any remaining water was then evaporated to determine the mass of the large particle fraction. The mass of the dissolved MMS was determined by difference and mixed with sufficient magnesium perchlorate to obtain a 1:1 ratio of salt to regolith analog in the slurry and thus in the particles nebulized.

These soil/salt solutions were nebulized using a Meinhard 500-μm orifice nebulizer. The nitrogen gas flows through the nebulizer at a 90°angle to the capillary tip, and the high velocity flow draws up the sample solution and breaks it into a particle mist, which is then deposited onto a hydrophobically coated fused silica disk. The resulting particles were an internal mixture of magnesium perchlorate and either the mineral or soil analog. The particles typically ranged from 5 to 50 μm in diameter, which corresponds to similar grain sizes on the surface of Mars (Dollfus & Deschamps, 1986).

Although we cannot say if the particles we generated are exactly a 1:1 salt to mineral (s) ratio, we assume that all particles were internally mixed because of the method in which they were generated. By internally mixed, we mean that within each particle (like the ones shown in Figure 3), there are magnesium perchlorate and mineral present, and the particles have the same salt : soil ratio as the solution from which they were generated. We also do not expect a dependence on the particle size because the particles that nucleated ice were different sizes for each experiment (due to the stochastic nature of ice nucleation) and each experiment resulted in only a small standard deviation.

Given the micrometer resolution of the Raman microscope, detailed observations of individual submicrometer grains in a mixed particle could not be probed. To ensure we started with dry particles, the sample was placed into an environmental cell within the Raman microscope and the particles were allowed to dry (no liquid water present in Raman spectrum) in a 0% $RH_{(l)}$ environment for approximately 5–10 min prior to beginning an experiment.

2.2. Surface and Mineral Analogs

In this study, a Mars-relevant mineral and a soil analog were used, which included sodium montmorillonite and MMS, respectively. Clay minerals are widespread on the surface and make up approximately 15–25% of the Martian surface (Bristow et al., 2017; Carter et al., 2015; Ehlmann & Edwards, 2014). Montmorillonite was chosen to represent the clay minerals found on the surface of Mars, since dioctehedral smectites are a common type of clay found. Frinak et al. (2005) studied the water uptake of montmorillonite and found that it took up a considerable amount of water, similar to that of very hygroscopic ammonium sulfate. The swelling nature of montmorillonite makes it an interesting candidate for studying the competition for water between the minerals and magnesium perchlorate. The second soil analog chosen to study the Martian regolith simulant MMS was first identified and characterized by Peters et al. (2008). MMS was used as a simulant for Mars global regolith because it is a good geochemical and mineralogical match to the Rocknest soil sample investigated by MSL and has low organic and water content. MMS is a combination of minerals and is mostly closely associated with plagioclase feldspar, Ca-rich pyroxene, and minor parts of magnetite. Table 1 shows the elemental composition of MMS (Peters et al., 2008). Ladino and Abbatt (2013) studied the ice nucleating ability of simulants MMS and JSC Mars-1 with relevance to Martian water ice clouds. That study found that MMS was better at nucleating ice than JSC Mars-1, a property that makes MMS an interesting candidate to mix with perchlorate salts and brines. In our studies, perchlorate brine will be supercooled or supersaturated in the presence of a soil analog to determine the effects on the DRH, ice formation, and ERH of pure perchlorate brines.

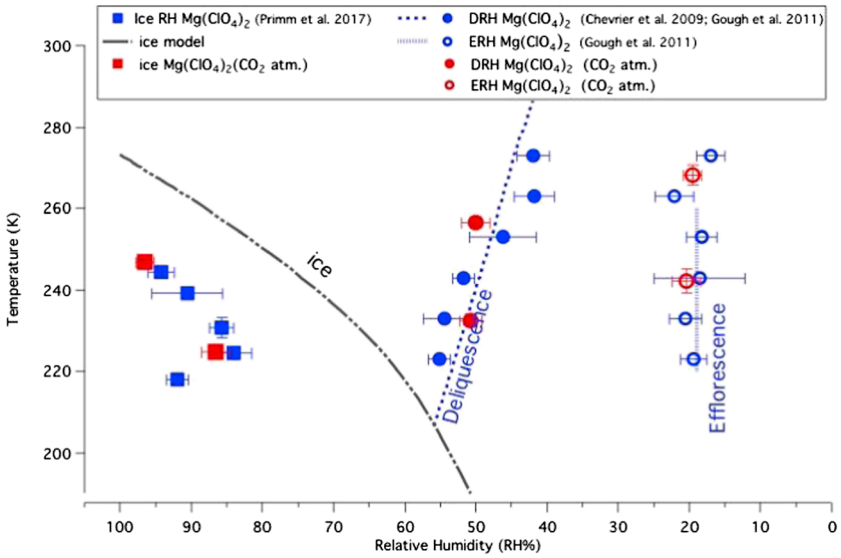

Figure 1. There are no detectable differences between the deliquescence relative humidity (RH), ice RH, and efflorescence RH of Mg $(ClO_4)_2 \cdot 6H_2O$ when an N_2 (blue markers) versus CO_2 atmosphere (red markers) is present.

2.3. Raman Microscope, Environmental Cell, and Flow System

A Raman microscope equipped with an environmental cell was used to identify the $RH_{(l)}$ and temperature conditions of ice formation, deliquescence, and efflorescence of each salt/mineral mixture. The experimental setup includes a Nicolet Almega XR Dispersive Raman spectrometer outfitted with a Linkam THMS600 environmental cell, a Linkam automated temperature controller, and a Buck Research chilled-mirror hygrometer. The environmental cell allows for $RH_{(l)}$ and temperature control. The phase transitions of individual particles were determined visually using the optical microscope and spectrally using Raman spectroscopy. This experimental setup has been described in more detail previously (Baustian et al., 2010; Gough et al., 2011; Schill & Tolbert, 2013).

While some precious experiments in this lab have varied the RH while keeping the temperature constant under a N_2 atmosphere, here we obtained S_{ice} and DRH values in these experiments by keeping using the same procedure. In both cases, the water vapor concentration was kept constant for the entire experiment by having a constant flow of CO_2 into a glass frit bubbler to produce humidified CO_2. While keeping the water vapor concentration constant throughout the experiment, the $RH_{(l)}$ was increased by lowering the temperature of the sample. After exiting the environmental cell, the flow of humidified CO_2 flowed into the CR-1A hygrometer where the dew/frost point temperature was measured. The opposite procedure was performed in order to obtain ERH values. The water vapor was kept constant, but the $RH_{(l)}$ was decreased by increasing the temperature until efflorescence was observed.

Previously in our lab, experiments in the Raman microscope flow system were performed using nitrogen as the flow gas. For the present work, we use CO_2 as the flow gas (Airgas Bone Dry 3.0 Grade) to make these studies more Mars-relevant. Prior to beginning the studies of mineral/salt mixtures, we performed experiments to determine the DRH, freezing, and ERH of pure Mg $(ClO_4)_2 \cdot 6H_2O$ under a CO_2 atmosphere and compared these values to the ones measured in a N_2 atmosphere, explained in section 3.1 and Figure 1.

2.4. Surface and Subsurface Modeling

At Gale Crater, the Rover Environmental Monitoring Station (REMS) has measured environmental conditions such as air temperature, ground temperature, RH with respect to ice, wind speed, and atmospheric pressure along Curiosity's traverse. Measurements are nominally taken during the first 5 min of each hour for more than two and a half Martian years at the time of this writing. Here we specifically use the ground temperature (T_g) measured by the ground temperature sensor, the air temperature measured at 1.6 m ($T_{1.6m}$) measured by multiple air temperature sensors, and the RH measured at 1.6 m ($RH_{1.6m}$) measured by a Vaisala RH sensor.

$T_{1.6m}$ and $RH_{1.6m}$ are used to find the water partial pressure at 1.6 m. This is assumed to be constant down to the surface, and then T_g is used to calculate the RH at the surface, RH_g.

In order to discard unreliable RH measurements affected by the heating of the sensor caused by the REMS control electronics, we select only those taken during the first 4 s following a period of at least 5 min of inactivity (Martínez et al., 2016). Reliable measurements are taken during both the nominal and high-resolution interval mode, which is typically used between 3 and 6 a.m. local time on 1- to 1-hr observation blocks and consists of alternately switching the sensor on and off at periodic intervals to minimize thermal contamination (Martínez et al., 2017). The average of the $RH_{1.6m}$ and $T_{1.6m}$ values measured during these 4 s is then calculated (measurements stay stable). To calculate RH_g, we consider quasi-simultaneous T_g values of the highest confident measured over a 5-min interval centered at the time at which RH measurements of the highest confidence are measured. This is done to avoid the noise in REMS T_g measurements and ensure a statistically robust T_g values. The data analysis strategy typically results in 24 hourly values of $RH_{1.6m}$ and $T_{1.6m}$, T_g, and RH_g per sol.

The Thermal and Electrical Conductivity Probe, or TECP, on the PHX lander measured the temperature, thermal conductivity, and volumetric heat capacity of the regolith (Zent et al., 2010). The TECP was mounted near the end of the 2.3-m robotic arm where it was able to measure the H_2O content of either the regolith or the air, depending on where it was positioned at the time. However, some in-soil measurements only measured temperature in-soil, while RH was measured in-air due to the location of the sensors. Furthermore, temperature was measured along the 15-mm length of the TECP needle, which is a nonnegligible fraction of the diurnal skin-depth (~5 cm) and therefore strongly affected by the temperature gradient in the regolith.

Subsurface temperature and RH conditions for both PHX and MSL were modeled using a 1-D, fully coupled, heat and mass transfer model with a vertical resolution of 0.01 m and small (180 s) temporal resolution that has been previously vetted for Mars (Chevrier & Rivera-Valentin, 2012; Kereszturi & Rivera-Valentin, 2012; Nuding et al., 2014; Rivera-Valentin et al., 2011). In the case of Gale crater, fits to REMS-derived water vapor pressure are applied as a boundary condition at the surface-atmosphere interface. The REMS measures, among other quantities, ground temperature and RH with respect to ice ($RH_{(i)}$) at 1.6 m (Hamilton et al., 2014; Harri et al., 2014). From these two quantities, the water vapor pressure can be derived. The TECP onboard PHX measured RH at various heights, but not consistently at the surface, making it difficult to integrate into the model (Zent et al., 2010, 2016). For PHX, the simulation includes an ice table at a depth of 0.1 m (Smith et al., 2009) that exchanges water vapor with the atmosphere. Thermal inertia for the regolith is consistent with site measurements at Gale Crater (Vasavada et al., 2017) and at the PHX landing site (Zent et al., 2010). Furthermore, perturbations to the water vapor mass flux through the regolith, such as adsorption or ice formation, are not considered.

3. Results

3.1. Effect of CO_2 Versus N_2 Atmosphere

Figure 1 shows the DRH, ERH, and S_{ice} values of pure Mg $(ClO_4)_2 \cdot 6H_2O$ measured in a CO_2 atmosphere compared to earlier work performed in a N_2 atmosphere. These data points are overlaid on the Mg $(ClO_4)_2$ + water stability diagram (Chevrier et al., 2009). The blue symbols represent phase transitions experimentally measured with N_2 as the carrier gas, and the red symbols represent phase transitions experimentally measured with CO_2 as the carrier gas. Atmospheric composition does not affect, within estimated uncertainties, the temperature or $RH_{(l)}$ conditions needed for the observed phase transitions of Mg $(ClO_4)_2 \cdot 6H_2O$ to occur. Because there is no significant difference within experimental uncertainty when N_2 or CO_2 are used, the phase transitions of pure Mg $(ClO_4)_2 \cdot 6H_2O$, which were performed under N_2 atmospheric conditions here and previously (Gough et al., 2011), can be confidently compared to studies performed in this paper under CO_2 atmospheric conditions.

3.2. Spectral Analysis

Montmorillonite and MMS have strong fluorescence signals in Raman spectra and are thus challenging to study using Raman spectroscopy. Species within minerals, such as transition metals, rare earth metals, and organic material, are known to fluoresce (Marshall & Olcott Marshall, 2015). However, MMS is a combination of minerals and the specific minerals of which it is composed are not well characterized. Nevertheless, MMS is

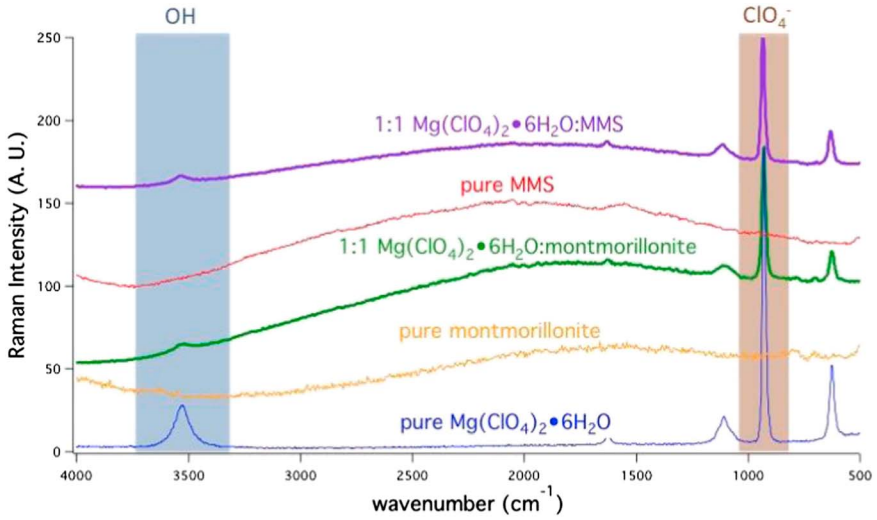

Figure 2. Raman spectra of pure Mg $(ClO_4)_2 \cdot 6H_2O$, pure montmorillonite, pure Mojave Mars Simulant (MMS), and 1:1 mixtures of perchlorate with montmorillonite or with MMS. The blue shaded region highlights the O–H stretch of water, and the brown shaded region highlights the ClO4– stretch.

red/brown in color, which shows that it absorbs visible green light, and montmorillonite is a gray color, meaning it also absorbs small amounts visible light. Both samples were collected from different locations on earth and could have trace amounts of biological material, which has conjugated pi-bonds known to absorb laser light and fluoresce. Here we treat the fluorescence itself as a spectral signature unique to the mineral, and therefore, we can identify a mixture of mineral and perchlorate based on the presence of a strong fluorescence background that raises the baseline (indicating a mineral) and a Raman stretch at 931 cm^{-1} (indicating magnesium perchlorate). Figure 2 shows Raman spectra of pure crystalline Mg $(ClO_4)_2 \cdot 6H_2O$, pure montmorillonite, and pure MMS as well as the 1:1 mixtures of Mg $(ClO_4)_2 \cdot 6H_2O$ with either montmorillonite or MMS. The OH stretch from the crystalline phase water in the hydrated magnesium perchlorate and also the perchlorate stretch from the salt are visible through the fluorescence from the mineral phase, confirming that the mixture particles indeed contain both species.

After the composition of a particle was analyzed at room temperature and $RH_{(l)}$~0%, the $RH_{(l)}$ was increased and the temperature was decreased until the particles were confirmed to have deliquesced visually and spectrally. These conditions were achieved by keeping the water vapor constant and decreasing the temperature. After a brine was formed, the temperature was further decreased to increase $RH_{(l)}$ until ice nucleation occurred and at least one of the brine droplets froze into a solid ice particle. This freezing could also be observed both visually and spectrally. After ice nucleation occurred, the temperature was increased to lower the $RH_{(l)}$ until melting occurred and then further lowered until efflorescence was observed. This entire procedure was repeated at least 3 times at 10–15 K temperature intervals within the range of 215 and 277 K.

3.3. Comparison of Pure Mg $(ClO_4)_2 \cdot 6H_2O$ to the Mixtures of Mg $(ClO_4)_2 \cdot 6H_2O$ With Montmorillonite and MMS

Figure 3 shows dry crystalline phase of pure Mg $(ClO_4)_2 \cdot 6H_2O$ particle (left, red curve) and that of a 1:1 Mg $(ClO_4)_2 \cdot 6H_2O$: montmorillonite mixture particle (right, red curve) deliquescing (blue curve), forming ice (green curve), and efflorescing (black curve). Raman spectra and corresponding microscope images are shown. While the particles and spectra look different with and without mineral, the features in the OH region (shaded in blue) 2,900–3,600 cm^{-1}, still clearly show the OH stretch of condensed-phase H_2O independent of composition of the particle. Before deliquescence (top red curve), the mixture particle has intense fluorescence as well as a visible O–H stretch of Mg $(ClO_4)_2 \cdot 6H_2O$. When the mixture particle deliquesces, the peak in the O–H stretching region broadens due to the formation of liquid water, similar to the spectral changes observed when pure Mg $(ClO_4)_2 \cdot 6H_2O$ deliquesces.

In Figure 3 at 223 K (blue curves), the pure Mg $(ClO_4)_2 \cdot 6H_2O$ particle deliquesced at 56% and the 1:1 Mg $(ClO_4)_2 \cdot 6H_2O$: montmorillonite mixture particle also deliquesced at 56%. When the $RH_{(l)}$ was increased

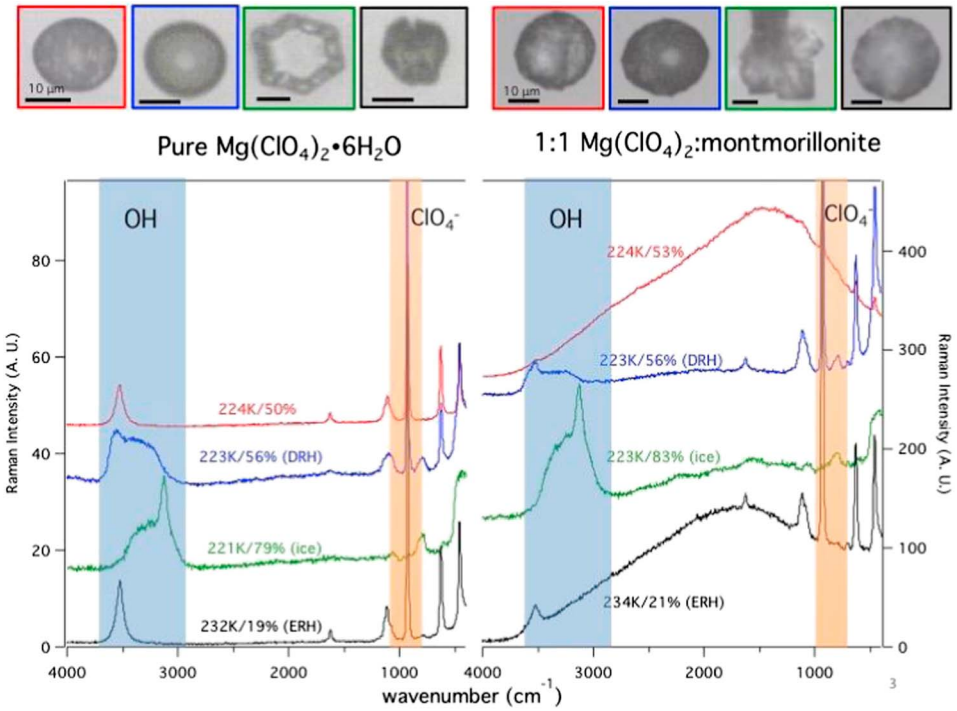

Figure 3. Raman spectra of pure Mg $(ClO_4)_2 \cdot 6H_2O$, pure montmorillonite, pure Mojave Mars Simulant (MMS), and 1:1 mixtures of perchlorate with montmorillonite or with MMS. The blue shaded region highlights the O–H stretch of water, and the brown shaded region highlights the ClO4– stretch.

further by decreasing the temperature to 222(±1) K, ice formation occurred at 79(±1)% $RH_{(I)}$ for pure Mg $(ClO_4)_2 \cdot 6H_2O$ and 83(±1)% $RH_{(I)}$ for the Mg $(ClO_4)_2 \cdot 6H_2O$: montmorillonite mixture. After ice formed, the $RH_{(I)}$ was decreased by increasing the temperature to 233(±1) K. The particle melted and finally effloresced into a crystalline particle at 19(±1)% $RH_{(I)}$ for pure Mg $(ClO_4)_2 \cdot 6H_2O$ and 21(±1)% $RH_{(I)}$ for the Mg $(ClO_4)_2 \cdot 6H_2O$: montmorillonite mixture. The three phase transitions (DRH, ice formation, and ERH) of the pure Mg $(ClO_4)_2 \cdot 6H_2O$ and Mg $(ClO_4)_2 \cdot 6H_2O$: montmorillonite mixture occurred within 4% $RH_{(I)}$ of each other, and thus, no significant difference was found between the behavior of the pure magnesium perchlorate particle and that of the mixture of perchlorate and montmorillonite. In all cases, the combination of images and spectra allowed for confident determination of the conditions for DRH, RH of ice formation, and ERH for the Mg $(ClO_4)_2 \cdot 6H_2O$/montmorillonite mixtures.

A similar analysis was performed using the 1:1 mixture of Mg $(ClO_4)_2 \cdot 6H_2O$ and MMS. Raman spectra of this mixture were not obtained because the MMS strongly absorbs 532-nm light (the excitation laser in the Raman spectrometer). We found that when a Raman spectrum was collected, the particle would absorb the laser light, heat up, and evaporate any liquid water. Unlike montmorillonite, which is light gray in color, the reddish MMS strongly absorbs 532-nm laser light. Because of this strong absorption, experiments were performed using only visual analysis. Crystalline dry particles have a structured, heterogeneous, light-colored visual appearance, while liquid particles are dark, homogeneous, and round. When the particle appeared rounder and darker, it had taken up water, and once all of the crystalline phase was dissolved, deliquescence had occurred. Once deliquescence is observed and the $RH_{(I)}$ is increased further, the particle started to nucleate ice when it appeared crystalline again and crystals started to grow outward. These visual clues also apply as the particle loses water. An example of this visual determination experiment for MMS is shown in Figure S2.

3.4. DRH, ERH, and Freezing Results for Mixtures of Mg $(ClO_4)_2 \cdot 6H_2O$ With Montmorillonite and MMS

Figure 4 shows the results of all deliquescence, ice formation, and efflorescence experiments performed on mixtures of 1:1 Mg $(ClO_4)_2 \cdot 6H_2O$: montmorillonite (part a) and 1:1 Mg $(ClO_4)_2 \cdot 6H_2O$: MMS (part b), as well as the individual pure components (perchlorate or mineral) for comparison. The experimental data are plotted

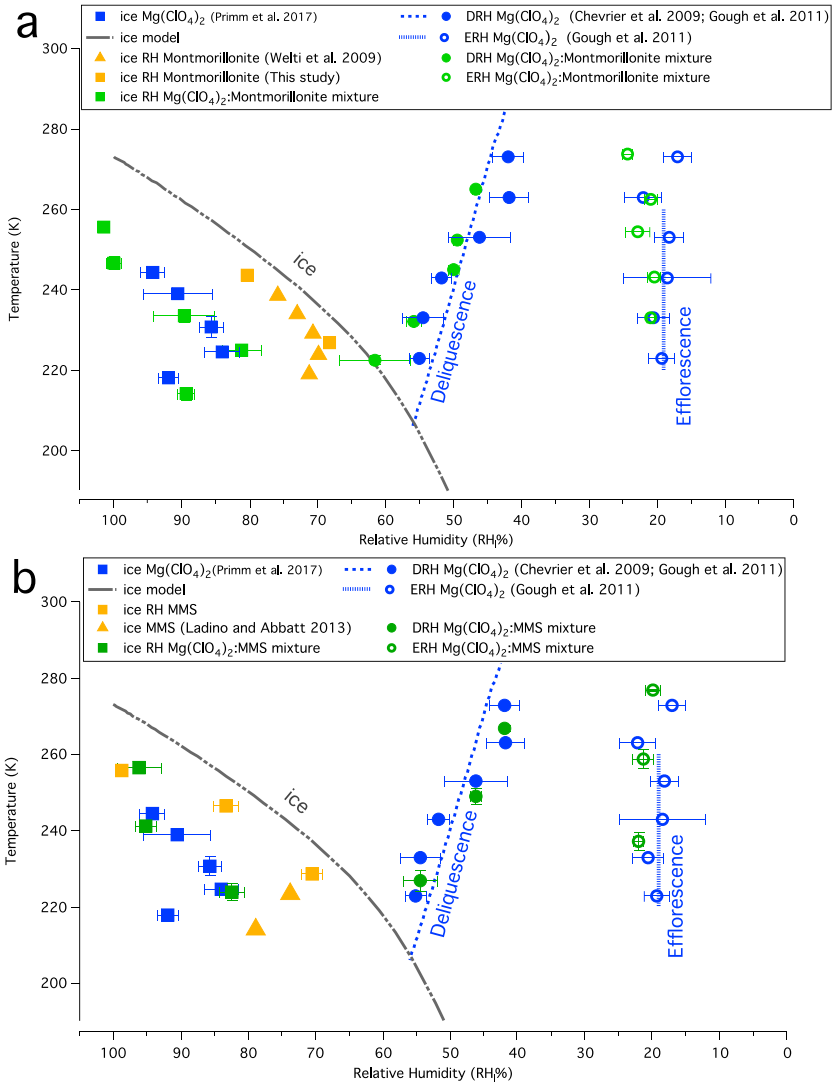

Figure 4. Plots showing the deliquescence relative humidity (RH), ice RH (S_{ice}), and efflorescence RH of pure Mg $(ClO_4)_2 \cdot 6H_2O$ and of 1:1 mixtures of perchlorate and mineral. (a) Mixtures of perchlorate with montmorillonite and (b) mixtures of perchlorate with Mojave Mars Simulant. Neither the mineral nor the regolith analog shows a significant effect on the deliquescence, efflorescence, or freezing phase transitions of perchlorate salt.

on the magnesium perchlorate-water stability diagram. The blue dotted deliquescence line is from a thermodynamic calculation (Chevrier et al., 2009), while the blue dashed efflorescence line is a best fit line. The blue symbols in both figures represent the experimentally determined deliquescence, efflorescence, or ice formation of pure perchlorate salt or brine (Gough et al., 2011; Primm et al., 2017) with standard deviations of the different experimental values. Because pure montmorillonite and MMS are insoluble materials, they have no DRH or ERH values. The ice nucleating ability of both montmorillonite and MMS has been studied (Ladino & Abbatt, 2013; Welti et al., 2009), and these S_{ice} values are shown as gold markers in both Figures 4a and 4b, where the squares represent experimental values performed in the this study and the triangles represent literature values. These ice formation values are plotted as $RH_{(l)}$ and not S_{ice} in order to reasonably plot them with DRH and ERH values. For reference, the black "ice" line is $S_{ice} = 1$. Both montmorillonite and MMS are efficient ice nuclei, nucleating ice when S_{ice} is close to one. Because Welti et al. (2009) studied ice nucleation by montmorillonite in a primarily N_2 atmosphere, we repeated this measurement in our Raman microscope with a CO_2 atmosphere (gold triangles in Figure 4a). Ladino and Abbatt (2013) studied the ice nucleation of MMS only at temperatures below 223 K (gold triangles in Figure 4b), and so we repeated the measurement of S_{ice} at a wider range of temperatures (gold squares).

In Figure 4a, the green symbols represent the observed phase transitions of Mg $(ClO_4)_2 \cdot 6H_2O$-montmorillonite mixtures, and in Figure 4b, the green symbols represent the observed phase transitions of Mg $(ClO_4)_2 \cdot 6H_2O$-MMS mixtures. It can be seen that neither montmorillonite nor MMS has an effect on the water uptake of pure Mg $(ClO_4)_2 \cdot 6H_2O$, within experimental standard deviation. For example, the DRH of pure Mg $(ClO_4)_2 \cdot 6H_2O$ at 233 K is 54.5 ± 2.3%, the DRH of the salt mixed with montmorillonite at the same temperature is 55.8 ± 1.1%, and the DRH of the salt mixed with MMS at 227 K is 54.4 ± 2.5%. To further analyze the differences in these numbers, we used a Student *t* test at 95% confidence and found that the difference is not significant. Similarly, beyond experimental uncertainty, there is no difference in ERH values between the pure salt and the salt-mineral mixture. The experimental $RH_{(l)}$ values at which ice was formed due to freezing of a brine had more scatter and standard deviation. This is likely due to the random nature of ice nucleation, and also because often only one particle on the entire sample would freeze initially. Despite this scatter, pure perchlorate brines and mixed perchlorate-mineral brines generally experienced the same extent of supercooling prior to freezing. The complete experimental data set plotted in Figure 4 is given in Table S1 in the supporting information, with the ice formation conditions reported as both $RH_{(l)}$ and S_{ice}.

4. Discussion

S_{ice} values as high as 1.45 were reached for the salt-mineral brine particles prior to freezing. This high value is surprising given the S_{ice} values for either pure mineral on its own close to 1.0. We found that the presence of the minerals, which are excellent ice nuclei, does not hinder the supercooling of the brine phase under high $RH_{(l)}$ and low *T* conditions that are predicted to form ice. Additionally, the minerals do not hinder supersaturation of the salt brine (ERH). When $RH_{(l)}$ values are lowered below the DRH, efflorescence of the salt-mineral mixture does not occur any more readily if mineral is present. This is also a surprising observation, as it is often assumed that the presence of an efficient ice nuclei, such as a mineral dust, will initiate precipitation of the solid salt. Our results suggest that not all potential nuclei will cause crystallization of a supersaturated salt solution. The reason why these minerals are not acting as good nucleation is unknown.

Bryant et al. (1960) proposed that the molecular level structures of the ice nuclei and of the salt can be correlated using the lattice mismatch between the two species. A lower lattice mismatch will theoretically result in nucleation occurring more readily, allowing less supersaturation of the brine phase. Davis et al. (2015) applied this theory to salt crystal efflorescence specifically. Here we use the methods of Davis et al. to calculate lattice mismatch values between Mg $(ClO_4)_2 \cdot 6H_2O$ and montmorillonite. The lattice mismatch equation is described in detail in Davis et al. (2015), but briefly, the equation is

$$\delta = \frac{\left|\frac{a_{\text{mineral}} - a_{\text{MP}}}{a_{\text{MP}}}\right| + \left|\frac{b_{\text{mineral}} - b_{\text{MP}}}{b_{\text{MP}}}\right|}{2}$$

where δ is the lattice mismatch value and *a* and *b* are cell parameters of the unit cell for a given species (mineral = montmorillonite or MMS; MP = Mg $(ClO_4)_2 \cdot 6H_2O$). The value of δ is calculated for each of the three different unit cell parameters, *a*, *b*, and *c*, and then these values can be compared between Mg $(ClO_4)_2 \cdot 6H_2O$ with MMS and montmorillonite (Davis et al., 2015; Kihara, 1990; Robertson & Bish, 2011). The lowest value is used to determine if there is a weak or strong lattice match. As stated in Davis et al., when $\delta \leq 0.12$, there is little lattice mismatch and so the mineral species is predicted to be effective at nucleating the supersaturated aqueous species, in this case Mg $(ClO_4)_2$. The lowest mismatch value with montmorillonite between the unit cell parameters was $\delta = 0.140$. This value suggests that Mg $(ClO_4)_2 \cdot 6H_2O$ and montmorillonite have different lattice structures, which could explain the ineffectiveness of recrystallization of the Mg $(ClO_4)_2$ solution by montmorillonite. From the high δ values, it can be seen that montmorillonite is a poor lattice match for crystalline perchlorate. This lattice mismatch could potentially explain why the ERH values of Mg $(ClO_4)_2 \cdot 6H_2O$ were unchanged even when the salt was mixed with montmorillonite. When the lattice mismatch was calculated between Mg $(ClO_4)_2$ and the components of MMS, the lowest δ value was 0.0487 for andesine, which comprised 41% of MMS. According to Davis et al. (2015), these two crystals should be a good enough match to promote nucleation, but no nucleation was promoted. However, recently, it has been shown that other crystalline species that have good lattice matches do not always cause nucleation (Ushijima et al., 2018). Thus, lattice mismatch calculation might not be the only factor for promoting nucleation.

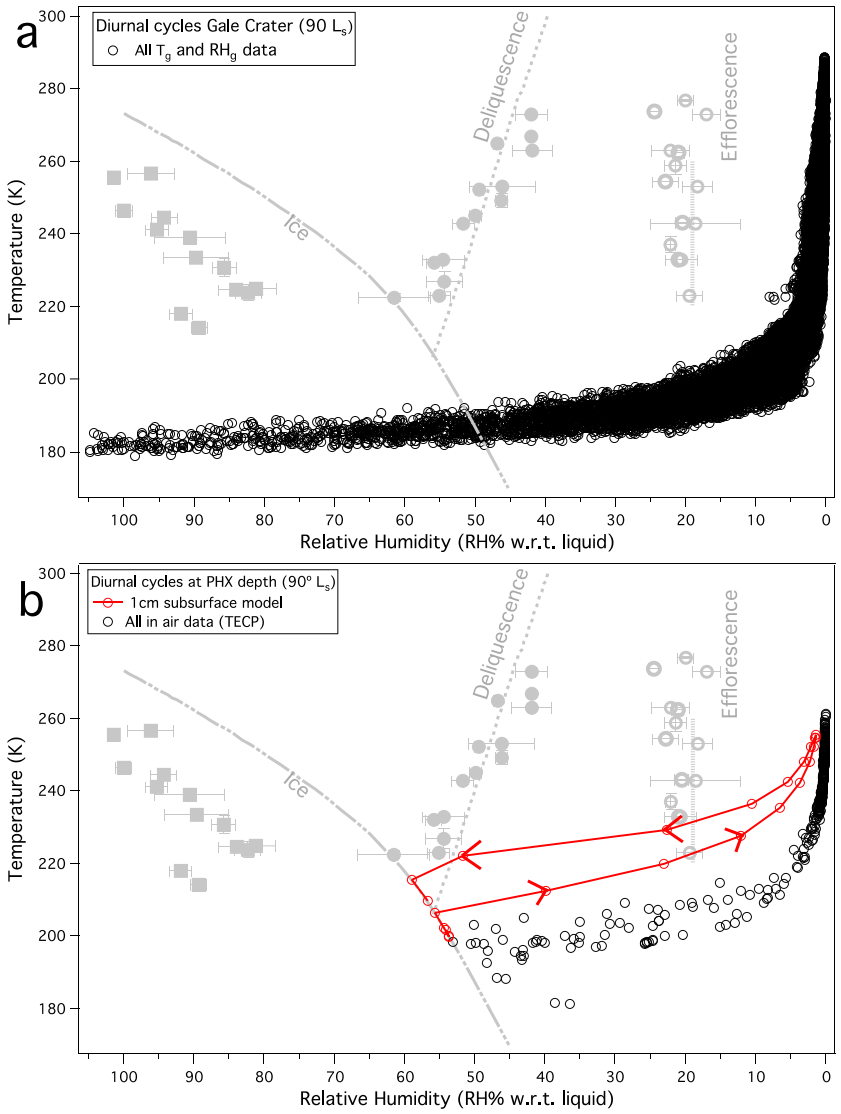

Figure 5. (a) Mars Science Laboratory Rover Environmental Monitoring Station data (black circles) and Gale Crater subsurface model results from different depths (colored lines, all $L = 90°$) overlaid on a magnesium perchlorate stability containing all experimental data from this paper (gray markers). (b) Phoenix Thermal and Electrical Conductivity Probe data (black circles) and Phoenix subsurface model results ($L = 90°$) overlaid on same stability diagram and data as (a). The red line represents the modeled subsurface conditions at 1-cm depth, and each open circle overlaying the red line represents 1 hr during this Martian sol.

The two materials (Mars-relevant mineral and soil analog) studied here are different in several ways. One is a swelling clay of singular mineralogy (montmorillonite), and the other is a mixture of several minerals that is not known to adsorb water vapor to a great extent (MMS). Despite these differences, they both had no effect on the phase transitions of magnesium perchlorate. According to Kiselev et al. (2017), ice nucleation occurs in defects on the surface of minerals, for example, steps, cracks, and cavities. These defects could serve as active sites to promote nucleation. It is possible that these defects on the mineral surface were deactivated or made inaccessible to water molecules in our experiments, and thus, nucleation was not promoted. If other Martian minerals and salts behave similarly, then previously published DRH and ERH values of pure Mars-relevant salts are still likely relevant to the real Martian environment, where salts and minerals are closely intermixed. This hypothesis along with the lattice mismatch calculations are just possible mechanisms to explain why MMS and montmorillonite did not cause any change in the nucleation of magnesium perchlorate; however, more work needs to be done to explain the physics of this nucleation behavior.

Because the surface of Mars is approximately 99% dust, it is important to recognize that our ratio of salt to mineral/regolith analog in the experiments is high (1:1) because of experimental limitations. Typical ice nuclei in the atmosphere that promote or initiate ice nucleation are generally smaller than that of the atmospheric droplet they come into contact with (Han & Martin, 1999). Martin et al. (2001) performed a study in which they increased the size of the mineral inclusion to observe the effect of the mineral inclusion on the ERH. An increase in the ERH was seen as the mineral inclusion diameter was increased from 60 to 450 nm. But, because the atmospheric droplet was around 1 μm in diameter, the mineral inclusion diameter was approximately 1 order of magnitude smaller than that of the atmospheric droplet it was inside of. Thus, it is possible for even small ratios of mineral dust : perchlorate to impact efflorescence.

5. Martian Implications: Potential for Deliquescence at Gale Crater (MSL) and Vastitas Borealis (PHX)

Although we found that neither montmorillonite nor MMS affected the perchlorate phase transition, other samples could still have an impact. Here we discuss the relevance for Mars, assuming that the behavior in actual surface soils is modeled well by our experiments, and perform this exercise for the surface using in situ data and the shallow subsurface using numerical modeling for Gale Crater, the landing site of the MSL and PHX landing sites.

Figure 5 shows measured and modeled RH and temperature data at Gale Crater (MSL) up to sol 1527 and Vastitas Borealis (PHX) overlaid on the Mg $(ClO_4)_2$ stability diagram. The data points representing the deliquescence, efflorescence, and freezing of Mg $(ClO_4)_2$, both pure and mixed with soil analogs, are included as gray points. Figure 5a shows all REMS RH_g and T_g data as black circles, and then modeled conditions at 1-cm depth as red and orange colored lines. In the case of these subsurface modeled conditions, the solar longitude (L_s) = 90°, which is shown here because the simulated diurnal cycle permits for the deliquescence of Mg $(ClO_4)_2$. Figure 5b shows all in-air data from the PHX TECP instrument averaged over 1-hr intervals (Zent et al., 2016). The measurement height varied, as the robotic arm of PHX was moved up and down over the course of the measurements. In Figure 5b, the modeled conditions at 1-cm depth are shown by the red line. Figure 5a shows that the conditions at MSL are too cold during high $RH_{(l)}$ periods for liquid Mg $(ClO_4)_2$ solutions to be possible, as the conditions do not cross the threshold of deliquescence of magnesium perchlorate (even mixed with minerals). Figure 5b shows that during some high $RH_{(l)}$ periods, the warm temperatures in the subsurface of the PHX landing site may allow for the deliquescence of magnesium perchlorate-soil/mineral analog mixtures. In laboratory experiments, our phase transitions occur within seconds (Davis & Tolbert, 2017) to minutes (this study) depending on temperature. Thus, for the subsurface at PHX, the modeled RH remains at favorable values long enough to allow for each phase transitions to occur (deliquescence, ice formation, and efflorescence). These findings are consistent with the suggestion of Cull et al. (2010) that the PHX landing site has had or currently has aqueous environments or thin liquid water films, which explains the transportation of perchlorate from the surface to the subsurface.

6. Conclusions

Since the finding of perchlorate and other soluble species in the Martian soil, interest in several laboratory experiments have probed brine stability and metastability. However, the surface of Mars is almost 99% mineral/mineral dust, and thus, the behavior of mixtures of brines with mineral dust must be considered. Experiments were performed investigating the potential effect of soil analogs on the deliquescence, efflorescence, and ice formation by the hygroscopic salt Mg $(ClO_4)_2 \cdot 6H_2O$. Particles of equal masses magnesium perchlorate and either sodium montmorillonite or MMS experienced deliquescence, ice formation, and efflorescence by varying temperature and RH.

In the atmospheric science community, it is well known that mineral dust and other insoluble mineral mixtures (similar to those found on the surface of Mars) serve as excellent ice nuclei, which could particularly affect processes involving supersaturation and supercooling. We observed, however, that the mineral had no detectable effect on any phase transitions of magnesium perchlorate. No significant difference was found in the water uptake and release (i.e., deliquescence, efflorescence, and ice formation) of a mars-relevant salt (magnesium perchlorate) mixed with a mineral found in the surface of Mars and a mars-relevant regolith analog, montmorillonite, and MMS, respectively. Particularly surprising is the inability of the soil analog to

affect the supersaturation of the salt that is observed when a brine is dehydrated or the supercooling of brine that occurs when ice is theoretically predicted to form. Our lattice mismatch calculations show that magnesium perchlorate and montmorillonite are not a good match for nucleation; thus, this could be an explanation for montmorillonite not efficiently promoting crystallization of magnesium perchlorate.

We have compared the stability diagrams of magnesium perchlorate mixed with Mars-relevant soil analogs to conditions found at the MSL and PHX landing sites. We find that the MSL landing site is not likely to have magnesium perchlorate brines because the ground temperatures during high RH periods are always below the eutectic temperature of the salt. At the PHX landing site, though, high RH periods during the summer are accompanied by temperatures above the eutectic temperature in the subsurface and are able to potentially generate a liquid phase if magnesium perchlorate is present, even if mixed with mineral soil analogs. These findings are consistent with several other studies on the presence of liquid at the PHX landing site (Cull et al., 2010; Fischer et al., 2014, 2016; Zorzano et al., 2009).

Author Disclosure Statement

No competing financial interests exist.

Acknowledgments
The data used are listed in the references, tables, figures, and supplements. This material is based upon work supported by the National Aeronautics and Space Administration under grant NNX14AJ96G and NASA Earth and Space Science Fellowship NNX15AT6OH. The authors would also like to thank Greg Peters at JPL for providing the MMS. E. G. Rivera-Valentin acknowledges support from the National Aeronautics and Space Administration under grant NNX15AM42G from the Mars Data Analysis Program.

References

Assemi, S., Sharma, S., Tadjiki, S., Prisbrey, K., Ranville, J., & Miller, J. D. (2015). Effect of surface charge and elemental composition on the swelling and delamination of montmorillonite nanoclays using sedimentation field-flow fractionation and mass spectroscopy. *Clays and Clay Minerals*, *63*(6), 457–468. https://doi.org/10.1346/CCMN.2015.0630604

Baustian, K. J., Wise, M. E., & Tolbert, M. A. (2010). Depositional ice nucleation on solid ammonium sulfate and glutaric acid particles. *Atmospheric Chemistry and Physics*, *10*, 2307–2317. https://doi.org/10.5194/acp-10-2307-2010

Bristow, T. F., Blake, D. F., Vaniman, D. T., Chipera, S. J., Rampe, E. B., Grotzinger, J. P., et al. (2017). Surveying clay mineral diversity in the Murray Formation, Gale Crater, Mars. *LPSC Abstract*, *48*, 9–10. Retrieved from https://ntrs.nasa.gov/search.jsp? R=20170001744

Bryant, G. W., Hallett, J., & Mason, B. J. (1960). The epitaxial growth of ice on single-crystalline substrates. *Journal of Physics and Chemistry of Solids*, *12*(2), 189–IN18. https://doi.org/10.1016/0022-3697(60)90036-6

Carter, J., Loizeau, D., Mangold, N., Poulet, F., & Bibring, J. (2015). Widespread surface weathering on early Mars: A case for a warmer and wetter climate. *Icarus*, *248*, 373–382. https://doi.org/10.1016/j.icarus.2014.11.011

Chevrier, V. F., Hanley, J., & Altheide, T. S. (2009). Stability of perchlorate hydrates and their liquid solutions at the Phoenix landing site, mars. *Geophysical Research Letters*, *36*, L10202. https://doi.org/10.1029/2009GL037497

Chevrier, V. F., & Rivera-Valentin, E. G. (2012). Formation of recurring slope lineae by liquid brines on present-day Mars. *Geophysical Research Letters*, *39*, L21202. https://doi.org/10.1029/2012GL054119

Cull, S. C., Arvidson, R. E., Catalano, J. G., Ming, D. W., Morris, R. V., Mellon, M. T., & Lemmon, M. (2010). Concentrated perchlorate at the Mars Phoenix landing site: Evidence for thin film liquid water on Mars. *Geophysical Research Letters*, *37*, L22203. https://doi.org/10.1029/2010GL045269

Cziczo, D. J., Froyd, K. D., Hoose, C., Jensen, E. J., Diao, M., Zondlo, M., et al. (2013). Clarifying the dominant sources and mechanisms of cirrus cloud formation. *Science*, *340*(6138), 1320–1324. https://doi.org/10.1126/science.1234145

Davis, R. D., Lance, S., Gordon, J. A., Ushijima, S. B., & Tolbert, M. A. (2015). Contact efflorescence as a pathway for crystallization of atmospherically relevant particles. *Proceedings of the National Academy of Sciences*, *112*(52), 15,815–15,820. https://doi.org/10.1073/pnas.1522860113

Davis, R. D., & Tolbert, M. A. (2017). Crystal nucleation initiated by transient ion-surface interactions at aerosol interfaces. *Science Advances*, *3*(7), e1700425. https://doi.org/10.1126/sciadv.1700425

Dollfus, A., & Deschamps, M. (1986). Grain-size determination at the surface of Mars. *Icarus*, *67*(1), 37–50. https://doi.org/10.1016/0019-1035(86)90172-7

Ehlmann, B. L., & Edwards, C. S. (2014). Mineralogy of the Martian surface. *Annual Review of Earth and Planetary Sciences*, *42*(1), 291–315. https://doi.org/10.1146/annurev-earth-060313-055024

Fischer, E., Martínez, G., Elliot, H. M., & Rennó, N. O. (2014). Experimental evidence for the formation of liquid saline water on Mars. *Geophysical Research Letters*, *41*, 4456–4462. https://doi.org/10.1002/2014GL060302.Received

Fischer, E., Martínez, G. M., & Rennó, N. O. (2016). Formation and persistence of brine on Mars: Experimental simulations throughout the diurnal cycle at the Phoenix landing site. *Astrobiology*, *16*(12), 937–948. https://doi.org/10.1089/ast.2016.1525

Frinak, E. K., Mashburn, C. D., Tolbert, M. A., & Toon, O. B. (2005). Infrared characterization of water uptake by low-temperature Na-montmorillonite: Implications for Earth and Mars. *Journal of Geophysical Research*, *110*, D09308. https://doi.org/10.1029/2004JD005647

Glavin, D. P., Freissinet, C., Miller, K. E., Eigenbrode, J. L., Brunner, A. E., Buch, A., et al. (2013). Evidence for perchlorates and the origin of chlorinated hydrocarbons detected by SAM at the Rocknest aeolian deposit in Gale Crater. *Journal of Geophysical Research: Planets*, *118*, 1955–1973. https://doi.org/10.1002/jgre.20144

Gough, R. V., Chevrier, V. F., Baustian, K. J., Wise, M. E., & Tolbert, M. A. (2011). Laboratory studies of perchlorate phase transitions: Support for metastable aqueous perchlorate solutions on Mars. *Earth and Planetary Science Letters*, *312*(3–4), 371–377. https://doi.org/10.1016/j.epsl.2011.10.026

Gough, R. V., Chevrier, V. F., & Tolbert, M. A. (2014). Formation of aqueous solutions on Mars via deliquescence of chloride-perchlorate binary mixtures. *Earth and Planetary Science Letters*, *393*, 73–82. https://doi.org/10.1016/j.epsl.2014.02.002

Hamilton, V. E., Vasavada, A. R., Sebastián, E., De La Torre Juárez, M., Ramos, M., Armiens, C., et al. (2014). Observations and preliminary science results from the first 100 sols of MSL Rover Environmental Monitoring Station ground temperature sensor measurements at Gale Crater. *Journal of Geophysical Research: Planets*, *119*, 745–770. https://doi.org/10.1002/2013JE004520

Han, J., & Martin, S. T. (1999). Heterogeneous nucleation of the efflorescence of (NH4)2SO4 particles internally mixed with AlzO3, TiOz, and ZrOz. *Journal of Geophysical Research*, *104*, 3543–3553. https://doi.org/10.1029/1998JD100072

Han, J. H., Hung, H. M., & Martin, S. T. (2001). The size effect of hematite and corundum inclusions on the efflorescence relative humidities of aqueous ammonium sulfate particles. *Geophysical Research Letters*, *28*, 2601–2604. https://doi.org/10.1029/2001GL013120

Harri, A., Genzer, M., Kemppinen, O., Haberle, R., Polkko, J., Savijärvi, H., et al. (2014). Mars Science Laboratory relative humidity observations: Initial results special section. *Journal of Geophysical Research: Planets*, *119*, 2132–2147. https://doi.org/10.1002/2013JE004514.Received

Hecht, M., Kounaves, S., Quinn, R., West, S., Young, S., Ming, D., et al. (2009). Detection of perchlorate and the soluble chemistry of Martian soil at the Phoenix Lander site. *Science*, *325*, 64–67. Retrieved from http://www.sciencemag.org/content/325/5936/64.short

Hoose, C., & Möhler, O. (2012). Heterogeneous ice nucleation on atmospheric aerosols: A review of results from laboratory experiments. *Atmospheric Chemistry and Physics*, *12*(20), 9817–9854. https://doi.org/10.5194/acp-12-9817-2012

Kereszturi, A., & Rivera-Valentin, E. G. (2012). Locations of thin liquid water layers on present-day Mars. *Icarus*, *221*(1), 289–295. https://doi.org/10.1016/j.icarus.2012.08.004

Kihara, K. (1990). An X-ray study of the temperature dependence of the quartz structure. *European Journal of Mineralogy*, *2*(1), 63–78. https://doi.org/10.1127/ejm/2/1/0063

Kiselev, A., Bachmann, F., Pedevilla, P., Cox, S. J., Michaelides, A., Gerthsen, D., & Leisner, T. (2017). Active sites in heterogeneous ice nucleation—The example of K-rich feldspars. *Science*, *355*(January), 367–371.

Ladino, L. a., & Abbatt, J. P. D. (2013). Laboratory investigation of Martian water ice cloud formation using dust aerosol simulants. *Journal of Geophysical Research: Planets*, *118*, 14–25. https://doi.org/10.1029/2012JE004238

Marion, G. M., Catling, D. C., Zahnle, K. J., & Claire, M. W. (2010). Modeling aqueous perchlorate chemistries with applications to Mars. *Icarus*, *207*(2), 675–685. https://doi.org/10.1016/j.icarus.2009.12.003

Marshall, C. P., & Olcott Marshall, A. (2015). Challenges analyzing gypsum on Mars by Raman spectroscopy. *Astrobiology*, *15*(9), 761–769. https://doi.org/10.1089/ast.2015.1334

Martínez, G. M., Fischer, E., Rennó, N. O., Sebastián, E., Kemppinen, O., Bridges, N., et al. (2016). Likely frost events at Gale crater: Analysis from MSL/REMS measurements. *Icarus*, *280*, 93–102. https://doi.org/10.1016/j.icarus.2015.12.004

Martínez, G. M., Newman, C. N., De Vicente-Retortillo, A., Fischer, E., Renno, N. O., Richardson, M. I., et al. (2017). The modern near-surface Martian climate: A review of in-situ meteorological data from Viking to Curiosity. *Space Science Reviews*, *212*(1–2), 339–340. https://doi.org/10.1007/s11214-017-0368-2

Navarro-González, R., Vargas, E., de la Rosa, J., Raga, A. C., & McKay, C. P. (2010). Reanalysis of the Viking results suggests perchlorate and organics at midlatitudes on Mars. *Journal of Geophysical Research*, *115*, E12010. https://doi.org/10.1029/2010JE003599

Nikolakakos, G., & Whiteway, J. A. (2015). Laboratory investigation of perchlorate deliquescence at the surface of Mars with a Raman scattering lidar. *Geophysical Research Letters*, *42*, 7899–7906. https://doi.org/10.1002/2015GL065434

Nikolakakos, G., & Whiteway, J. A. (2018). Laboratory study of adsorption and deliquescence on the surface of Mars. *Icarus*, *308*, 221–229. https://doi.org/10.1016/j.icarus.2017.05.006

Nuding, D. L., Rivera-Valentin, E. G., Davis, R. D., Gough, R. V., Chevrier, V. F., & Tolbert, M. A. (2014). Deliquescence and efflorescence of calcium perchlorate: An investigation of stable aqueous solutions relevant to Mars. *Icarus*, *243*, 420–428. https://doi.org/10.1016/j.icarus.2014.08.036

Ojha, L., Wilhelm, M. B., Murchie, S. L., Mcewen, A. S., Wray, J. J., Hanley, J., et al. (2015). Spectral evidence for hydrated salts in recurring slope lineae on Mars. *Nature Geoscience*, *8*(11), 829–832. https://doi.org/10.1038/NGEO2546

Pant, A., Parsons, M. T., & Bertram, A. K. (2006). Crystallization of aqueous ammonium sulfate particles internally mixed with soot and kaolinite: Crystallization relative humidities and nucleation rates. *Journal of Physical Chemistry A*, *110*(28), 8701–8709. https://doi.org/10.1021/jp060985s

Pestova, O. N., Myund, L. A., Khripun, M. K., & Prigaro, A. V. (2005). Polythermal study of the systems M (ClO4)2-H2O (M2+ = Mg2+, Ca2+, Sr2+, Ba2+). *Russian Journal of Applied Chemistry*, *78*(3), 409–413. https://doi.org/10.1007/s11167-005-0306-z

Peters, G. H., Abbey, W., Bearman, G. H., Mungas, G. S., Smith, J. A., Anderson, R. C., et al. (2008). Mojave Mars simulant—Characterization of a new geologic Mars analog. *Icarus*, *197*(2), 470–479. https://doi.org/10.1016/j.icarus.2008.05.004

Primm, K. M., Gough, R. V., Chevrier, V. F., & Tolbert, M. A. (2017). Freezing of perchlorate and chloride brines under Mars-relevant conditions. *Geochimica et Cosmochimica Acta*, *212*, 211–220. https://doi.org/10.1016/j.gca.2017.06.012

Reid, J. P., & Sayer, R. M. (2003). Heterogeneous atmospheric aerosol chemistry: Laboratory studies of chemistry on water droplets. *Chemical Society Reviews*, *32*(2), 70–79. https://doi.org/10.1039/b204463n

Rivera-Valentin, E. G., Blackburn, D. G., & Ulrich, R. (2011). Revisiting the thermal inertia of Iapetus: Clues to the thickness of the dark material. *Icarus*, *216*(1), 347–358. https://doi.org/10.1016/j.icarus.2011.09.006

Robertson, K., & Bish, D. (2011). Stability of phases in the Mg (ClO4)2-nH2O system and implications for perchlorate occurrences on Mars. *Journal of Geophysical Research*, *116*, E07006. https://doi.org/10.1029/2010JE003754

Schill, G. P., & Tolbert, M. A. (2013). Heterogeneous ice nucleation on phase-separated organic-sulfate particles: effect of liquid vs. glassy coatings. *Atmospheric Chemistry and Physics*, *13*, 4681–4695. https://doi.org/10.5194/acp-13-4681-2013

Smith, P. H., Tamppari, L. K., Arvidson, R. E., Bass, D., Blaney, D., Boynton, W. V., et al. (2009). H_2O at the Phoenix landing site. *Science 325*, 58–61.

Toner, J. D., Catling, D. C., & Light, B. (2014). The formation of supercooled brines, viscous liquids, and low-temperature perchlorate glasses in aqueous solutions relevant to Mars. *Icarus*, *233*, 36–47. https://doi.org/10.1016/j.icarus.2014.01.018

Toner, J. D., Catling, D. C., & Light, B. (2015). A revised Pitzer model for low-temperature soluble salt assemblages at the Phoenix site, Mars. *Geochimica et Cosmochimica Acta*, *166*, 327–343. https://doi.org/10.1016/j.gca.2015.06.011

Ushijima, S. B., Davis, R. D., & Tolbert, M. A. (2018). Immersion and contact efflorescence induced by mineral dust particles. *Journal of Physical Chemistry A*, *122*(5), 1303–1311. https://doi.org/10.1021/acs.jpca.7b12075

Vasavada, A. R., Piqueux, S., Lewis, K. W., Lemmon, M. T., & Smith, M. D. (2017). Thermophysical properties along Curiosity's traverse in Gale crater, Mars, derived from the REMS ground temperature sensor. *Icarus*, *284*, 372–386. https://doi.org/10.1016/j.icarus.2016.11.035

Welti, A., Lüönd, F., Stetzer, O., & Lohmann, U. (2009). Influence of particle size on the ice nucleating ability of mineral dusts. *Atmospheric Chemistry and Physics*, 6705–6715. Retrieved from http://www.atmos-chem-phys.net/9/6705/

Zent, A. P., Hecht, M. H., Cobos, D. R., Wood, S. E., Hudson, T. L., Milkovich, S. M., et al. (2010). Initial results from the Thermal and Electrical Conductivity Probe (TECP) on phoenix. *Journal of Geophysical Research*, *115*, E00E14. https://doi.org/10.1029/2009JE003420

Zent, A. P., Hecht, M. H., Hudson, T. L., Wood, S. E., & Chevrier, V. F. (2016). A revised calibration function and results for the Phoenix mission TECP relative humidity sensor. *Journal of Geophysical Research: Planets*, *121*, 626–651. https://doi.org/10.1002/2015JE004933

Zorzano, M.-P., Mateo-Martí, E., Prieto-Ballesteros, O., Osuna, S., & Renno, N. (2009). Stability of liquid saline water on present day Mars. *Geophysical Research Letters*, *36*, L20201. https://doi.org/10.1029/2009GL040315